Published in final edited form as:
J Cell Biochem. 2011 January ; 112(1): 118–127. doi:10.1002/jcb.22896.

Role of Bim in diallyl trisulfide-induced cytotoxicity in human cancer cells

Byeong-Chel Lee[1], **Bae-Hang Park**[1], **Seog-Young Kim**[2], and **Yong J. Lee**[2,3,*]

[1] Department of Medicine, School of Medicine, University of Pittsburgh, Pittsburgh, Pennsylvania 15213, USA

[2] Department of Surgery, School of Medicine, University of Pittsburgh, Pittsburgh, Pennsylvania 15213, USA

[3] Department of Pharmacology & Chemical Biology, School of Medicine, University of Pittsburgh, Pittsburgh, Pennsylvania 15213, USA

Abstract

The aim of this study was to investigate the effect of garlic constituent diallyl trisulfide (DATS) on the cell death signaling pathway in a human breast cell line (MDA-MB-231). We observed that DATS (10–100 μM) treatment resulted in a dose- and time-dependent cytotoxicity. Treatment of MDA-MB-231 cells with a cytotoxicity inducing concentration of DATS (50–80 μM) resulted in an increase in the intracellular level of reactive oxygen species (ROS). Data from assay with MitoSOX™ Red reagent suggest that mitochondria are the main source of ROS generation during DATS treatment. DATS-induced oxidative stress was detected through glutaredoxin (GRX), a redox-sensing molecule, and subsequently GRX was dissociated from apoptosis signal-regulating kinase 1 (ASK1). Dissociation of GRX from ASK1 resulted in the activation of ASK1. ASK1 activated a downstream signal transduction JNK (C-Jun N-terminal kinase)-Bim pathway. SP600125, a JNK inhibitor, inhibited DATS-induced Bim phosphorylation and protected cells from DATS-induced cytotoxicity. Our results indicate that the cytotoxicity caused by DATS is mediated by the generation of ROS and subsequent activation of the ASK1-JNK-Bim signal transduction pathway in human breast carcinoma MDA-MB-231 cells.

Keywords

Diallyl trisulfide; reactive oxygen species; ASK1; JNK; Bim

INTRODUCTION

Breast cancer has become the most frequently diagnosed cancer among women in the United States and the second most frequent cause of cancer death [Jemal et al., 2006]. Even though early diagnosis of breast cancer with mammography has improved over the last ten years, the optimal management of this disease remains undefined. When breast cancers progress to an advanced stage, treatment options are limited and are associated with significant morbidity and mortality. Since a multi-step progression from small, low-grade lesions to large, high-grade and metastatic carcinomas is involved in tumorigenicity as well as tumor

[*]All correspondence should be addressed to Dr. Yong J. Lee, Department of Surgery, University of Pittsburgh, Hillman Cancer Center, 5117 Centre Ave. Room 1.46C, Pittsburgh, PA 15213, U.S.A., Tel (412) 623–3268, Fax (412) 623–7709, leeyj@upmc.edu.

growth and metastasis, one strategy to deal with breast cancer is the blockage of a stage of this process with chemoprevention agents.

A relationship between consumption of *allium* vegetables (e.g., leeks, chives, onions, garlic, etc.) and cancer reduction has been demonstrated by epidemiological studies [Gao et al., 1999]. The curative agent has been localized to the primary sulfur compound, γ-glutamyl cysteine, which generates alliin (S-alkenyl-L-cysteine sulfoxide), the precursor of the organosulfur compounds (OSCs) which include diallyl sulfide (DAS), diallyl disulfide (DADS), and DATS [Fleischauer et al., 2000]. Among these, DATS is known to be the most effective antitumor agent [Xiao et al., 2004], and the effect of this oil-soluble compound has been extensively studied [Stan and Singh, 2009; Zhang et al., 2009; Wu et al., 2009]. DATS has been found to induce growth arrest and apoptotic death in a variety of tumor cell types [Zhang et al., 2009; Wu et al., 2009; Singh et al., 2008; Xiao et al., 2009; Shankar et al., 2008]. Although the antitumorigenic effect of DATS has been well established, the mechanisms underlying such apoptotic death are not completely understood.

Previous studies reveal that differential modulation of reactive oxygen intermediates (ROI) and mitochondria membrane potential (MMP) may account for the apoptotic effects of DATS [Das et al., 2007; Kim et al., 2007]. The underlying hypothesis driving this study is that DATS elevates the intracellular level of ROS and redox-regulatory proteins such as thioredoxin (TRX) and GRX recognize DATS-induced oxidative stress and activate the ASK1-MEK-JNK-Bim signal transduction pathway. Bim is a link in the ASK1-MEK-JNK-Bim signal transduction pathway which triggers apoptosis through the Bax-dependent mitochondrial apoptotic pathway. It is possible that Bim is activated during DATS treatment to transmit the cytotoxic effects of DATS treatment for breast cancer—that is the subject of this study.

Bim functions as part of the ASK1-JNK-Bim signal transduction pathway. This pathway can be activated by redox-regulatory proteins such as TRX and GRX when these proteins recognize ROS. We hypothesize that the intracellular level of ROS is elevated by DATS when DATS is applied to treat breast cancer cells, ultimately activating the ASK1-JNK-Bim signal transduction pathway. This overall schema is suggested because it has been found that DATS produces a differential modulation of ROI correlated with downstream changes in MMP and increased apoptosis [Das et al., 2007; Kim et al., 2007].

As the result of our efforts, presented here, we are able to state that DATS induces ROS which is recognized by GRX to activate the ASK1-JNK-Bim signal transduction pathway. This is evidenced by the fact that cytotoxicity is reduced during DATS application when specific JNK inhibitor SP600125 is applied, resulting in the inhibition of Bim.

MATERIALS AND METHODS

Cell culture

Human breast carcinoma MDA-MB-231 cells are estrogen receptor negative, p53-mutant and highly metastatic breast cancer cells. Mycoplasma infection is not detected with MycoFluorTM Mycoplasma Detection Kit (Molcular Probes, Invitrogen, Carlsbad, CA). Cells were cultured in Dulbecco's modified Eagle's medium (DMEM) with 10% fetal bovine serum (FBS) (HyClone, Logan, UT, USA) and 26 mM sodium bicarbonate for monolayer cell culture. The cells were maintained in a humidified atmosphere containing 5% CO_2 and air at 37°C.

Drug treatment

DATS and SP600125 (a JNK inhibitor) were purchased from LKT Laboratories (St. Paul, MN, USA) and Sigma-Aldrich (St. Louis, MO, USA), respectively. These drugs were prepared and dissolved in dimethylsulphoxide (DMSO) and applied to cells. Treatment of cells with drugs was accomplished by aspirating the medium and replacing it with medium containing these drugs.

Determination of cell viability

One or two days prior to the experiment, cells were plated into 60-mm Petri dishes at a density of 1×10^5 cells per plate in 5 ml tissue culture medium in triplicate. For trypan blue exclusion assay, trypsinized cells were pelleted and resuspended in 0.2 ml of medium, 0.5 ml of 0.4% trypan blue solution and 0.3 ml of phosphate-buffered saline solution (PBS). The samples were mixed thoroughly, incubated at room temperature for 15 min, and examined under a light microscope. At least 300 cells were counted for each survival determination. For the morphological evaluation of cell death, cells were treated and then analyzed by phase-contrast microscopy.

Measurement of ROS generation

ROS generation in control and DATS-treated cells was measured by flow cytometry following staining with 2′,7′-dichlorofluorescein diacetate (DCFH-DA) (Molecular Probes, Invitrogen). Briefly, MDA-MB-231 cells were seeded in six-well plates (1×10^5 cells per well), allowed to attach overnight and exposed to DMSO (control) or desired concentrations of DATS for specified time periods. The cells were stained with 20 μM DCFH-DA for 30 min at 37°C, and the fluorescence was detected by a fluorescence microscope. Alternatively, the fluorescence intensity of dichlorofluorescein in cells was determined using the flow cytometer (Becton Dickinson and Co., Rockville, MD, USA).

Mitochondrial assays

Mitochondrial ROS levels were quantified as described by the manufacturer (Molecular Probes, Invitrogen). MDA-MB-231 cells were seeded into 60-mm Petri dishes two days prior to the experiments. Cells were treated with desired concentrations of DATS or 100 μM H_2O_2 for 1 h. Before harvesting, cells were incubated with 5 μM MitoSOX™ Red reagent (Molecular Probes, Invitrogen) for 10 min. Cells were washed with PBS, collected, and kept on ice in the dark for immediate detection with a flow cytometer (Coulter Epics XL flow cytometer).

Adenovirus vectors

Adenoviral vector containing HA-tagged ASK1 (Ad.HA-ASK1) or His-tagged GRX (Ad.His-GRX) was constructed as described previously [Song et al., 2002]. In brief, all recombinant adenoviruses were constructed by employing the *Cre-lox* recombination system [Hardy et al., 1997]. The selective cell line, CRE8, has a β-actin-based expression cassette driving a *Cre* recombinase gene with an NH_2-terminal nuclear localization signal stably integrated into 293 cells. Cells (5×10^5) were plated into a six-well plate 1 day before transfection. For the production of recombinant adenovirus, CRE8 cells were cotransfected with shuttle vector and ψ 5 viral genomic DNA by using LipofectAMINE Reagent (Invitrogen, Carlsbad, CA, USA). The recombinant adenoviruses were generated by intermolecular homologous recombination between the shuttle vector and ψ5 viral DNA. The new virus had an intact packaging site and carried a recombinant gene. Plaques were harvested, analyzed, and purified. The insertion of HA-ASK1 or His-GRX to adenovirus was confirmed by western blot analysis after infection of the corresponding recombinant

adenovirus into MDA-MB-231 cells. The adenovirus containing human catalase was kindly provided by B. Davidson (University of Iowa).

Antibodies

Anti-JNK antibody was purchased from Santa Cruz (Santa Cruz, CA, USA), anti-phosphorylated JNK, anti-phospho-Bim and anti-Bim antibody were from Cell Signaling (Beverly, MA, USA), anti-HA (clone 3F10) from Roche Diagnostics (Mannheim, Germany), anti-His (penta-His; mouse) from Qiagen (Valencia, CA, USA), and anti-actin antibody from ICN (Costa Mesa, CA, USA).

Protein extracts and polyacrylamide gel electrophoresis (PAGE)

Cells were lysed with Laemmli lysis buffer (2.4 M glycerol, 0.14 M Tris, pH 6.8, 0.21 M sodium dodecyl sulfate (SDS), 0.3 mM bromophenol blue) and boiled for 10 min. Protein content was measured with BCA Protein Assay Reagent (Pierce, Rockford, IL, USA). The samples were diluted with lysis buffer containing 1.28 M β-mercaptoethanol, and equal amounts of protein were loaded on 8–12% SDS–polyacrylamide gels. SDS–PAGE analysis was performed according to Laemmli [1970] using a Hoefer gel apparatus.

Immunoblot analysis

Proteins were separated by SDS–PAGE and electrophoretically transferred to nitrocellulose membrane. The nitrocellulose membrane was blocked with 5% non-fat dry milk in PBSTween-20 (0.1%, v/v) at 4°C overnight. The membrane was incubated with primary antibody (diluted according to the manufacturer's instructions) for 2–16 h. Horseradish peroxidase conjugated anti-rabbit or anti-mouse IgG was used as the secondary antibody. Immunoreactive protein was visualized by the chemiluminescence protocol (ECL, Amersham, Arlington Heights, IL, USA). Quantitation of X-ray film was carried out by scanning and followed by analysis with an image program.

Interaction between proteins

For immunoprecipitation, cells were lysed in buffer containing 150 mM NaCl, 20 mM Tris-HCl (pH 7.5), 10 mM EDTA, 1% Triton X-100, 1% deoxycholate, 1 mM phenylmethylsulfonyl fluoride (PMSF), protein inhibitor cocktail solution (Sigma-Aldrich), and then the lysates were incubated with 1 μg of anti-penta-His mouse IgG1 (Qiagen) for 2 h. After the addition of protein-G agarose (Santa Cruz), the lysates were incubated an additional 2 h. The beads were washed three times with lysis buffer, separated by SDS-PAGE, and immunoblotted.

RESULTS

DATS induces cytotoxicity in human breast cancer cells

To investigate morphological changes, human breast carcinoma MDA-MB-231 cells were treated with 0–100 μM DATS for 16 h or 50 μM DATS for various times (0–24 h) and then observed under a light microscope and photographed. Observations made under the microscope showed that, after DATS treatment, the cell number decreased in dose- and time-dependent manner and, more interestingly, the shape of the cells changed in comparison to control cells (Fig. 1A and 1B). Apoptotic cell death, which is associated with typical morphological features like cell shrinkage and cytoplasmic membrane blebbing, was observed. We further examined the effect of various concentrations of DATS on cell viability. Data from trypan blue exclusion assay show that DATS treatment resulted in a dose-dependent decrease in the viability until 50 μM dose and then no further cytotoxicity

was observed (Fig. 1C). Unlike DATS, DMSO caused little or no cytotoxicity (data not shown).

Generation of ROS during treatment with DATS

To examine the mechanism of DATS-induced cytotoxicity, we measured the intracellular level of ROS during treatment with DATS by using DCFH-DA, which has been shown to be relatively specific for H_2O_2. H_2O_2 is able to oxidize DCFH to the fluorescent DCF. DCF fluorescence signals were detected with a fluorescence microscope (Fig. 2A) and measured using a flow cytometer (Fig. 2C). Figure 2A shows that significant fluorescence signals were observed in cells which were exposed to H_2O_2 or DATS, but not untreated control cells. Similar results were obtained with a flow cytometer (Fig. 2C). The oxidation of DCFH-DA was dependent upon DATS dose (Fig. 2B). To examine whether mitochondria are the main source of ROS generation during DATS treatment, cells were stained with MitoSOX™ Red reagent which is a fluorogenic dye for highly selective detection of superoxide in the mitochondria. Figure 3 shows that significant signals were detected in 50 μM DATS treated cells. These results suggest that DATS generates ROS through the mitochondria.

Activation of ASK1 during treatment with DATS

Next, we examined whether DATS-induced ROS activates ASK1, upstream of JNK, which is known to be associated with cell death. Previous studies illustrate that oxidative stress can be detected through redox-sensing molecules including TRX and GRX. These molecules bind to ASK1 and suppress its activation. It is well known that both GRX and TRX contain two redox-active half-cystine residues, -Cys-Gly-Pro-Cys- or –Cys-Pro-Tyr-Cys-, in an active center [Holmgren, 1989; Padilla et al., 1995]. These molecules form an intramolecular disulfide bond between cysteine residues in the oxidizing environment [Chrestensen et al., 1995; Song and Lee, 2003]. Formation of an intramolecular disulfide bond leads to a conformational change and subsequently results in dissociation of TRX and GRX from ASK1 [Yang et al., 1998; Zheng et al., 1998]. To investigate this possibility, MDA-MB-231 cells were coinfected with adenoviral vector containing His-tagged GRX (Ad.His-GRX) and HA-tagged ASK1 (Ad.HA-ASK1) and then exposed to various concentrations (10 and 80 μM) of DATS for 1 h. The interaction between ASK1 and GRX was evaluated by immunoprecipitation assay (Fig. 4A) and the ratio of ASK and GRX was quantitated (Fig. 4B). Figure 4 shows that GRX dissociated from ASK1 during treatment with DATS. To investigate the involvement of ROS in the dissociation GRX from ASK1, cells were coinfected with adenoviral vector containing catalase (Ad.Catalase). Figure 4 shows that dissociation of GRX from ASK1 during 10 μM DATS treatment was suppressed by Ad.Catalase infection. However, less suppression was observed during treatment with 80 μM DATS. This is probably due to the high concentration of DATS.

Activation of the JNK-Bim signal transduction pathway during treatment with DATS

It is well known that ASK1 is a member of the mitogen-activated protein kinase kinase kinase family that activates the JNK pathways by directly phosphorylating and thereby activating its respective mitogen-activated protein kinase kinases, MKK4/7 and MKK3/6 [Takekawa et al., 2005; Song and Lee, 2005]. We examined whether ASK1 activates the JNK pathway during treatment with DATS. Figure 5B shows that DATS treatment induces the activation (phosphorylation) of JNK and its downstream molecule Bim_{EL}. Previous studies have shown that JNK phosphorylates Bim which is known to be involved in Bax oligomerization and subsequently results in cytochrome *c* release. Indeed, we observed that phosphorylation of Bim_{EL} occurred during treatment with DATS (Fig. 5B). DATS treatment resulted in a dose-dependent phosphorylation of Bim_{EL}. Unlike DATS, DMSO alone did not significantly induce phosphorylation of JNK and Bim_{EL} (Fig. 5A).

JNK inhibitor suppresses DATS-induced Bim phosphorylation and protects cells from DATS-induced cytotoxicity

We hypothesize that JNK-mediated Bim phosphorylation potentiates Bax oligomerization, resulting in cytochrome *c* release and cytotoxicity. To test the hypothesis, we pretreated cells with JNK inhibitor SP600125 and then treated with DATS in the presence of SP600125. Figure 6A clearly demonstrates that DATS-induced phosphorylation of JNK and Bim was inhibited by treatment with SP600125. DATS-induced changes in morphological shape (Fig. 6B) and viability (Fig. 6C) were protected by treatment with SP600125. These results suggest that DATS-induced activation of the JNK-Bim signal transduction pathway plays an important role in DATS-induced cytotoxicity.

DISCUSSION

In this study, we examined the cytotoxic mechanism of one potential chemoprevention agent, DATS, which is a constituent of *allium* vegetables. DATS concentrations that significantly decrease human breast carcinoma MDA-MB-231 cell viability have similar effects on other cancer cell cultures, such as lung [Wu et al., 2009], prostate [Xiao et al., 2004], and colon [Hosono et al., 2005]. These observations suggest that DATS can be used as a chemoprevention agent for a variety of cancers.

Our studies and literatures demonstrate that DATS functions as a chemoprevention agent by inducing apoptosis of tumor cells through the generation of ROS which creates oxidative stress (Figs. 1 and 2) [Das et al., 2007,Kim et al., 2007,Antosiewicz et al., 2006,Xiao et al., 2005]. Although ROS may be generated both by organellar sources (mitochondrial electron transport chain and peroxisomal cytochrome P-450 oxidases) and endogenous enzyme systems (plasma membrane NADPH oxidase and cytoplasmic xanthine oxidase) [Gamaley and Klyubin, 1999], our data suggest that the mitochondria are the main source of ROS generation during DATS treatment (Fig. 3). Other agents have also been found to generate ROS through the mitochondria, notably DATS in human prostate cancer [Kim et al., 2007], and several chemopreventive agents such as benzyl isothiocyanate, phenethyl isothiocyanate, and sulforaphane through inhibiting complex I or III of the mitochondrial respiratory chain and disrupting the mitochondrial membrane potential [Xiao et al., 2008;Xiao et al., 2006;Singh et al., 2005]. During mitochondrial respiration, O_2 acts as the terminal acceptor of electrons, with the 4-electron reduction of O_2 yielding H_2O. In normal tissue, this has been estimated to occur at least 96–99% of the time. However, it is possible for a one-electron reduction of O_2 to yield superoxide, probably in the electron transport chain at Site I (NADH-dehydrogenase) or Site III (ubiquinone-cytochrome b) [Boveris and Cadenas, 1982]. Manganese superoxide dismutase (MnSOD) catalyzes this superoxide to dismute to H_2O_2 and O_2. The H_2O_2 is detoxified to H_2O and O_2 either by glutathione peroxidase in the mitochondria, or, if it diffuses into the cytosol, by catalase in peroxisomes. It is possible that DATS-induced elevation of the intracellular level of ROS is due to disruption of mitochondrial electron transport chain activity and/or the downstream glutathione peroxidase/glutathione reductase system. This possibility needs to be investigated in the future studies.

Our data demonstrate that treatment activates the JNK-associated signal transduction pathway through redox-sensing molecules including GRX (Figs. 4 and 5). In the oxidizing environment created by ROS, TRX and GRX dissociate from ASK1, an upstream protein in the JNK-associated signal transduction pathway, causing activation of the pathway [Saitoh et al., 1998;Song et al., 2002]. In a non-oxidizing environment, TRX and GRX bind to the N-terminal or C-terminal portion of ASK1, respectively [Saitoh et al., 1998;Song et al., 2002], but TRX and GRX contain two redox-active half-cystine residues, -Cys-Pro-Tyr-Cys- or -Cys-Gly-Pro-Cys-, in an active center [Holmgren, 1989;Padilla et al., 1995], and,

under oxidizing conditions, an intramolecular disulfide bond forms, for both TRX and GRX according to some investigators, between the cysteine residues leading to a conformational change and subsequently resulting in dissociation of TRX and GRX from ASK1, a dissociation which activates the ASK1-MEK-JNK signal transduction pathway [Saitoh et al., 1998;Song et al., 2002]. Previously we observed differential roles for TRX and GRX in oxidative stress-induced ASK-1 activation [Song and Lee, 2003], raising the possibility that GRX may activate ASK1 by a way other than through the mitochondria. Unlike TRX, GRX is highly selective for glutathione-containing mixed disulfides, and its catalytic cycle involves a covalent glutathionyl-enzyme disulfide intermediate (GRX-SSG) rather than an intramolecular disulfide at its active site [Yang et al., 1998]. GRX may recognize DATS-induced oxidative stress through catalytic reactions with oxidized glutathione (GSSG), forming GRX-SSG which is interconverted between GRX-SSG and an intramolecular disulfide form of GRX (GRX-[S-S]) by side reaction [Yang et al., 1998]. The oxidized GRX, GRX-SSG or GRX-[S-S], would then dissociate from ASK1 resulting in the activation of ASK1.

After DATS treatment produces ROS which causes dissociation of TRX and GRX from ASK and subsequently activation of ASK1, ASK1 activates JNK and leads to apoptotic death. This is plausible because ASK1 is a MAPK kinase kinase which can activate both the SAPKs (via activation of MKK4/7) and the p38 MAPKs (via activation of MKK3/6) [Ichijo et al., 1997], and previous studies suggest that sustained activation of the JNK signal causes apoptosis [Tobiume et al., 2001]. After being activated, JNK may phosphorylate Bim, a member of the BH-3 only proapoptotic subfamily of the Bcl-2 protein family, to cause apoptosis. This occurs because JNK's phosphorylation of Bim, in the non-transient Bim_L and Bim_{EL} isoforms [O'Reilly et al., 2000], interferes with Bim's dynein light chain (DLC) binding motif and prevents the suppression of Bim's apoptotic function, which under normal conditions is sequestered to the dynein motor complex by binding with the dynein light chain LC8/DLC1 [Lei and Davis, 2003; Puthalakath et al., 1999]. After JNK phosphorylation, phosphorylated Bim may activate Bax to activate the mitochondrial pathway [Lei and Davis, 2003; Putcha et al., 2001].

In this paper, we present the possibility that the cytotoxic mechanism of DATS operates through production of ROS which causes activation of the ASK1-MEK-JNK-Bim pathway and subsequently the Bax-dependent mitochondrial apoptotic pathway. Our model can be used in future studies of these linkages.

Acknowledgments

This work was supported by the following grants: NCI grant funds (CA121395 and CA140554), and Susan G. Komen Breast Cancer Foundation fund (BCTR60306).

Abbreviations used in this paper

Ad.Catalase	adenoviral vector containing catalase
Ad.HA-ASK1	adenoviral vector containing HA-tagged ASK1
Ad.His-GRX	adenoviral vector containing His-tagged GRX
ASK1	apoptosis signal-regulating kinase 1
DADS	diallyl disulfide
DAS	diallyl sulfide
DATS	diallyl trisulfide

DCFH-DA	2′,7′-dichlorofluorescein diacetate
DLC1	dynein light chain 1
DMEM	Dulbecco's modified Eagle's medium
DMSO	dimethylsulphoxide
FBS	fetal bovine serum
GRX	glutaredoxin
GSSG	oxidized glutathione
JNK	c-Jun N-terminal kinase
MMP	mitochondria membrane potential
MOI	multiplicity of infection
OSC	organosulfur compound
PAGE	polyacrylamide gel electrophoresis
PBS	phosphate-buffered saline
PMSF	phenylmethylsulfonyl fluoride
ROI	reactive oxygen intermediates
ROS	reactive oxygen species
SDS	sodium dodecyl sulfate
TRX	thioredoxin

References

Antosiewicz J, Herman-Antosiewicz A, Marynowski SW, Singh SV. c-Jun NH(2)-terminal kinase signaling axis regulates diallyl trisulfide-induced generation of reactive oxygen species and cell cycle arrest in human prostate cancer cells. Cancer Res. 2006; 66:5379–5386. [PubMed: 16707465]

Boveris, A.; Cadenas, E. Production of superoxide radicals and hydrogen peroxide in mitochondria. In: Oberley, LW., editor. Superoxide Dismutase. Vol. II. Boca Raton, FL: CRC Press Inc; 1982. p. 15-30.

Chrestensen CA, Eckman CB, Starke DW, Mieyal JJ. Cloning, expression, and characterization of human thioltransferase (Glutaredoxin) in *E. coli*. FEBS Lett. 1995; 374:25–28. [PubMed: 7589505]

Das A, Banik NL, Ray SK. Garlic compounds generate reactive oxygen species leading to activation of stress kinases and cysteine proteases for apoptosis in human glioblastoma T98G and U87MG cells. Cancer. 2007; 110:1083–1095. [PubMed: 17647244]

Fleischauer AT, Poole C, Arab L. Garlic consumption and cancer prevention: meta-analyses of colorectal and stomach cancers. Am J Clin Nutr. 2000; 72:1047–1052. [PubMed: 11010950]

Gamaley IA, Klyubin IV. Roles of reactive oxygen species: signaling and regulation of cellular functions. Int Rev Cytol. 1999; 188:203–238. [PubMed: 10208013]

Gao CM, Takezaki T, Ding JH, Li MS, Tajima K. Protective effect of allium vegetables against both esophageal and stomach cancer: a simultaneous case-referent study of a high-epidemic area in Jiangsu Province, China. Jpn J Cancer Res. 1999; 90:614–621. [PubMed: 10429652]

Hardy S, Kitamura M, Harris-Stansil T, Dai Y, Phipps ML. Construction of adenovirus vectors through Cre-lox recombination. J Virol. 1997; 71:1842–1849. [PubMed: 9032314]

Holmgren A. Thioredoxin and glutaredoxin systems. J Biol Chem. 1989; 264:13963–13966. [PubMed: 2668278]

Hosono T, Fukao T, Ogihara J, Ito Y, Shiba H, Seki T, Ariga T. Diallyl trisulfide suppresses the proliferation and induces apoptosis of human colon cancer cells through oxidative modification of beta-tubulin. J Biol Chem. 2005; 280:41487–41493. [PubMed: 16219763]

Ichijo H, Nishida E, Irie K, ten Dijke P, Saitoh M, Moriguchi T, Takagi M, Matsumoto K, Miyazono K, Gotoh Y. Induction of apoptosis by ASK1, a mammalian MAPKKK that activates SAPK/JNK and p38 signaling pathways. Science. 1997; 275:90–94. [PubMed: 8974401]

Jemal A, Siegel R, Ward E, Murray T, Xu J, Smigal C, Thun MJ. Cancer statistics. CA Cancer J Clin. 2006; 56:106–130. [PubMed: 16514137]

Kim YA, Xiao D, Xiao H, Powolny AA, Lew KL, Reilly ML, Zeng Y, Wang Z, Singh SV. Mitochondria-mediated apoptosis by diallyl trisulfide in human prostate cancer cells is associated with generation of reactive oxygen species and regulated by Bax/Bak. Mol Cancer Ther. 2007; 6:1599–1609. [PubMed: 17513609]

Laemmli UK. Cleavage of structural proteins during the assembly of the head of bacteriophage T4. Nature. 1970; 227:680–685. [PubMed: 5432063]

Lei K, Davis RJ. JNK phosphorylation of Bim-related members of the Bcl2 family induces Bax-dependent apoptosis. Proc Natl Acad Sci U S A. 2003; 100:2432–2437. [PubMed: 12591950]

O'Reilly LA, Cullen L, Visvader J, Lindeman GJ, Print C, Bath ML, Huang DC, Strasser A. The proapoptotic BH3-only protein bim is expressed in hematopoietic, epithelial, neuronal, and germ cells. Am J Pathol. 2000; 157:449–461. [PubMed: 10934149]

Padilla CA, Martinez-Galiseo E, Barcena JA, Spyrou G, Holmgren A. Purification from placenta, amino acid sequence, structure comparisons and cDNA cloning of human glutaredoxin. Eur J Biochem. 1995; 227:27–34. [PubMed: 7851394]

Putcha GV, Moulder KL, Golden JP, Bouillet P, Adams JA, Strasser A, Johnson EM. Induction of BIM, a proapoptotic BH3-only BCL-2 family member, is critical for neuronal apoptosis. Neuron. 2001; 29:615–628. [PubMed: 11301022]

Puthalakath H, Huang DC, O'Reilly LA, King SM, Strasser A. The proapoptotic activity of the Bcl-2 family member Bim is regulated by interaction with the dynein motor complex. Mol Cell. 1999; 3:287–296. [PubMed: 10198631]

Saitoh M, Nishitoh H, Fujii M, Takeda K, Tobiume K, Sawada Y, Kawabata M, Miyazono K, Ichijo H. Mammalian thioredoxin is direct inhibitor of apoptosis signal-regulating kinase (ASK) 1. EMBO J. 1998; 17:2596–2606. [PubMed: 9564042]

Shankar S, Chen Q, Ganapathy S, Singh KP, Srivastava RK. Diallyl trisulfide increases the effectiveness of TRAIL and inhibits prostate cancer growth in an orthotopic model: molecular mechanisms. Mol Cancer Ther. 2008; 7:2328–2338. [PubMed: 18723480]

Singh SV, Powolny AA, Stan SD, Xiao D, Arlotti JA, Warin R, Hahm ER, Marynowski SW, Bommareddy A, Potter DM, Dhir R. Garlic constituent diallyl trisulfide prevents development of poorly differentiated prostate cancer and pulmonary metastasis multiplicity in TRAMP mice. Cancer Res. 2008; 68:9503–9511. [PubMed: 19010926]

Singh SV, Srivastava SK, Choi S, Lew KL, Antosiewicz J, Xiao D, Zeng Y, Watkins SC, Johnson CS, Trump DL, Lee YJ, Xiao H. Herman-Antosiewicz A. Sulforaphane-induced cell death in human prostate cancer cells is initiated by reactive oxygen species. J Biol Chem. 2005; 280:19911–19924. [PubMed: 15764812]

Song JJ, Lee YJ. Differential role of glutaredoxin and thioredoxin in metabolic oxidative stress-induced activation of apoptosis signal-regulating kinase 1. Biochem J. 2003; 373:845–853. [PubMed: 12723971]

Song JJ, Lee YJ. Dissociation of Akt1 from its negative regulator JIP1 is mediated through the ASK1-MEK-JNK signal transduction pathway during metabolic oxidative stress: a negative feedback loop. J Cell Biol. 2005; 170:61–72. [PubMed: 15998799]

Song JJ, Rhee JG, Suntharalingam M, Walsh SA, Spitz DR, Lee YJ. Role of glutaredoxin in metabolic oxidative stress: glutaredoxin as a sensor of oxidative stress mediated by H_2O_2. J Biol Chem. 2002; 277:46566–46575. [PubMed: 12244106]

Stan SD, Singh SV. Transcriptional repression and inhibition of nuclear translocation of androgen receptor by diallyl trisulfide in human prostate cancer cells. Clin Cancer Res. 2009; 15:48895–4903.

Tobiume K, Matsuzawa A, Takahashi T, Nishtoh H, Morita K, Takeda K, Minowa O, Miyazono K, Noda T, Ichijo H. ASK1 is required for sustained activation of JNK/p38 MAP kinases and apoptosis. EMBO reports. 2001; 2:222–228. [PubMed: 11266364]

Wu XJ, Hu Y, Lamy E, Mersch-Sundermann V. Apoptosis induction in human lung adenocarcinoma cells by oil-soluble allyl sulfides: triggers, pathways, and modulators. Environ Mol Mutagen. 2009; 50:266–275. [PubMed: 19197990]

Xiao D, Choi S, Johnson DE, Vogel VG, Johnson CS, Trump DL, Lee YJ, Singh SV. Diallyl trisulfide-induced apoptosis in human prostate cancer cells involves c-Jun N-terminal kinase and extracellular-signal regulated kinase-mediated phosphorylation of Bcl-2. Oncogene. 2004; 23:5594–5606. [PubMed: 15184882]

Xiao D, Herman-Antosiewicz A, Antosiewicz J, Xiao H, Brisson M, Lazo JS, Singh SV. Diallyl trisulfide-induced G(2)-M phase cell cycle arrest in human prostate cancer cells is caused by reactive oxygen species-dependent destruction and hyperphosphorylation of Cdc 25 C. Oncogene. 2005; 24:6256–6268. [PubMed: 15940258]

Xiao D, Lew KL, Zeng Y, Xiao H, Marynowski SW, Dhir R, Singh SV. Phenethyl isothiocyanate-induced apoptosis in PC-3 human prostate cancer cells is mediated by reactive oxygen species-dependent disruption of the mitochondrial membrane potential. Carcinogenesis. 2006; 27:2223–2234. [PubMed: 16774948]

Xiao D, Powolny AA, Singh SV. Benzyl isothiocyanate targets mitochondrial respiratory chain to trigger reactive oxygen species-dependent apoptosis in human breast cancer cells. J Biol Chem. 2008; 283:30151–20163. [PubMed: 18768478]

Xiao D, Zeng Y, Hahm ER, Kim YA, Ramalingam S, Singh SV. Diallyl trisulfide selectively causes Bax- and Bak-mediated apoptosis in human lung cancer cells. Environ Mol Mutagen. 2009; 50:201–212. [PubMed: 18800351]

Yang Y, Jao SC, Nanduri S, Starke D, Mieyal JJ, Qin J. Reactivity of the human thioltransferase (glutaredoxin) C7S, C25S, C78S, C82S mutant and NMR solution structure of its glutathionyl mixed disulfide intermediate reflect catalytic specificity. Biochemistry. 1998; 37:17145–17156. [PubMed: 9860827]

Zhang YK, Zhang XH, Li JM, Sun de S, Yang Q, Diao DM. A proteomic study on a human osteosarcoma cell line Saos-2 treated with diallyl trisulfide. 2009; 20:702–712.

Zheng M, Aslund F, Storz G. Activation of the OxyR transcription factor by reversible disulfide bond formation. Science. 1998; 279:1718–1721. [PubMed: 9497290]

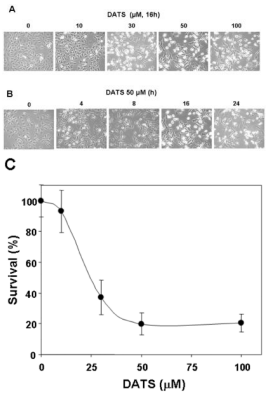

Figure 1. DATS induces cytotoxicity in human breast carcinoma MDA-MB-231 cells

Cells were treated with various concentrations (0–100 μM) for 16 h (**A** and **C)** or 50 μM DATS for various times (0–24 h) (**B**). **A** and **B:** Morphological features of each cell were analyzed with a phase-contrast inverted microscope. **C:** After DATS treatment, the cytotoxic effects of DATS were determined using the trypan blue exclusion assay. Error bars represent SEM from triplicate experiments.

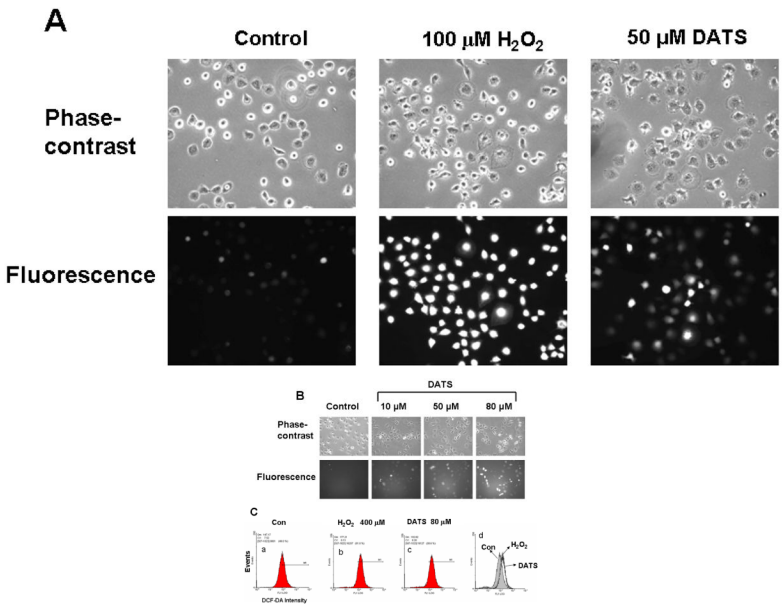

Figure 2. DATS treatment induces ROS generation in MDA-MB-231 cells

(A) Cells were treated with either 100 μM H_2O_2 or 50 μM DATS for 1 h. **(B)** Cells were treated with various concentrations (10–80 μM) of DATS for 1 h. Hydrogen peroxide generation was measured by incubation with 20 μM fluorescence probe DCFH-DA for 30 min using a fluorescence microscope. Control: untreated cells. **(C)** As an alternative way of measurement of hydrogen peroxide generation, flow cytometry was used. After H_2O_2/DATS-treated MDA-MB-231 cells were incubated with 20 μM fluorescence probe DCFH-DA for 30 min, stained cells were analyzed with a FACscan flow cytometer. Data from panels a, b, and c were summarized in panel d. Con: untreated cells.

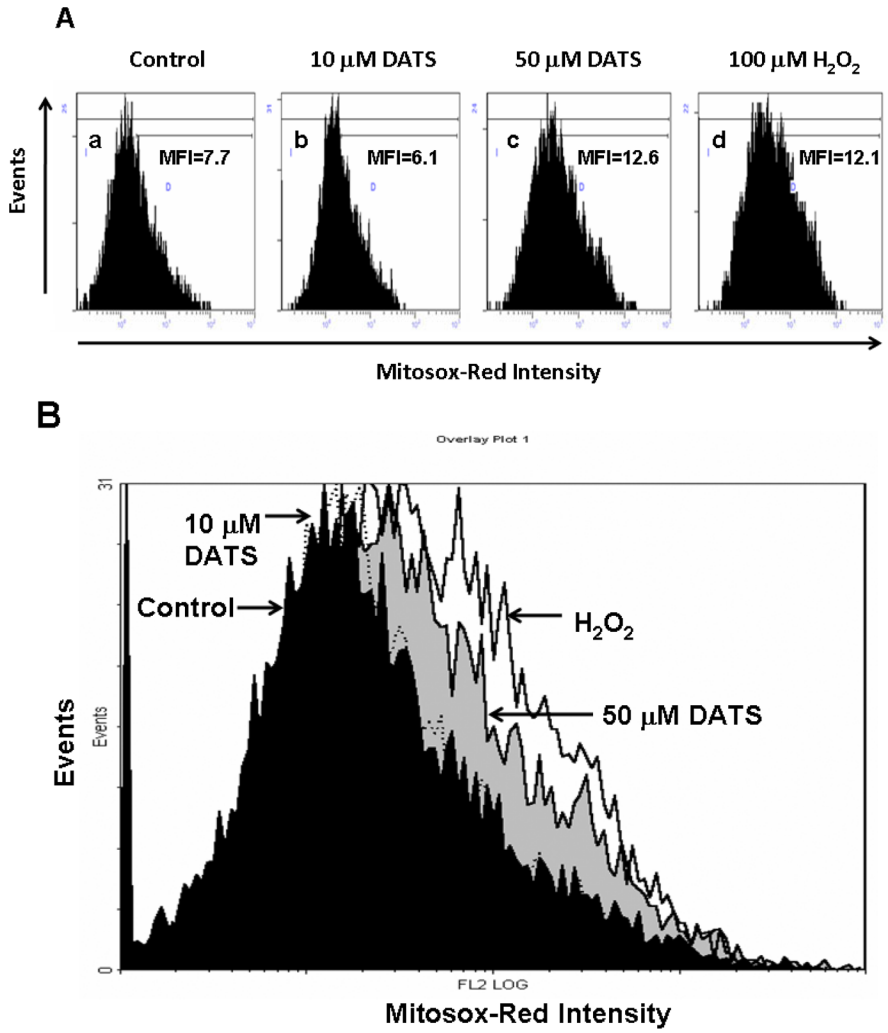

Figure 3. Measurement of mitochondrial ROS during DATS treatment

(A) To measure mitochondrial ROS, MDA-MB-231 cells were treated with DATS (10 or 50 μM) or 100 μM H_2O_2 for 1 h, and stained with 5 μM MitoSOX™ Red for 10 min. Stained cells were analyzed with a flow cytometer. Control: untreated cells. **(B)** Data from panels a, b, c and d were summarized.

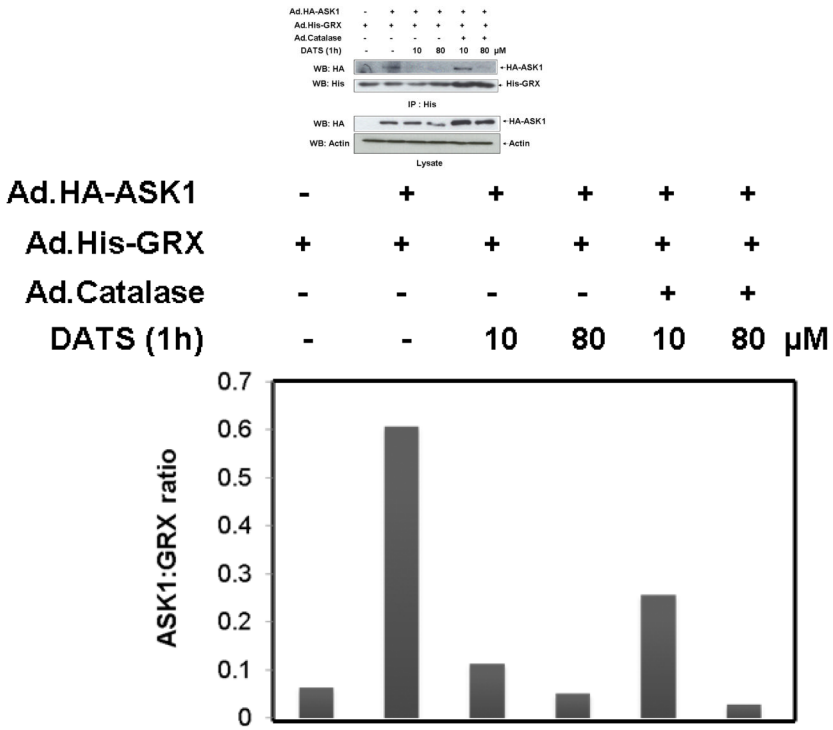

Figure 4. Effect of DATS on the interaction between GRX and ASK1 in MDA-MB-231 cells

(A) Cells were coinfected with adenoviral vectors containing His-tagged GRX (Ad.His-glutaredoxin, 30 MOI), HA-tagged ASK1 (Ad.HA-ASK1, 5 MOI), and catalase (Ad.Catalase, 10 MOI). After 24 h of incubation, cells were treated with DATS (10 or 80 μM) for 1 h. Cell lysates were divided into two fractions. One fraction of lysates was immunoprecipitated with 2 μg of His antibody, and then immunoblotted with anti-HA antibody or anti-His antibody. The other fraction of lysates was immunoblotted with anti-HA antibody. Actin was used to confirm that similar amounts of proteins were loaded in each lane. **(B)** The ratio of ASK1:GRX for each experimental group was plotted.

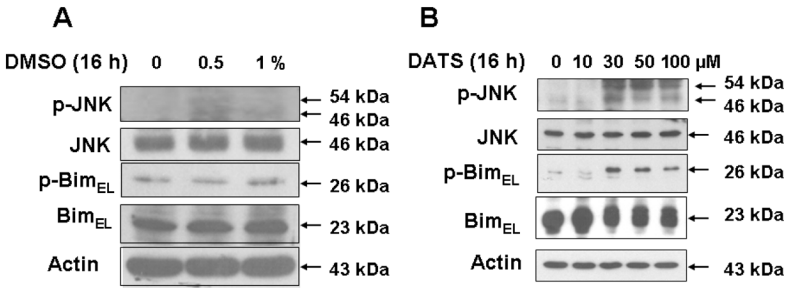

Figure 5. DATS treatment induces the JNK-Bim signal transduction pathway in MDA-MB-231 cells

(A) Cells were treated with various concentrations of DMSO (0.5–1%) for 16 h and then harvested. **(B)** Cells were treated with various concentrations of DATS (10–100 μM) for 16 h and then harvested. Equal amounts of protein (20 μg) were separated by SDS-PAGE and immunoblotted with anti-phospho-JNK, anti-JNK, anti-phospho-Bim, and anti-Bim antibody. Actin was used to confirm that similar amounts of proteins were loaded in each lane.

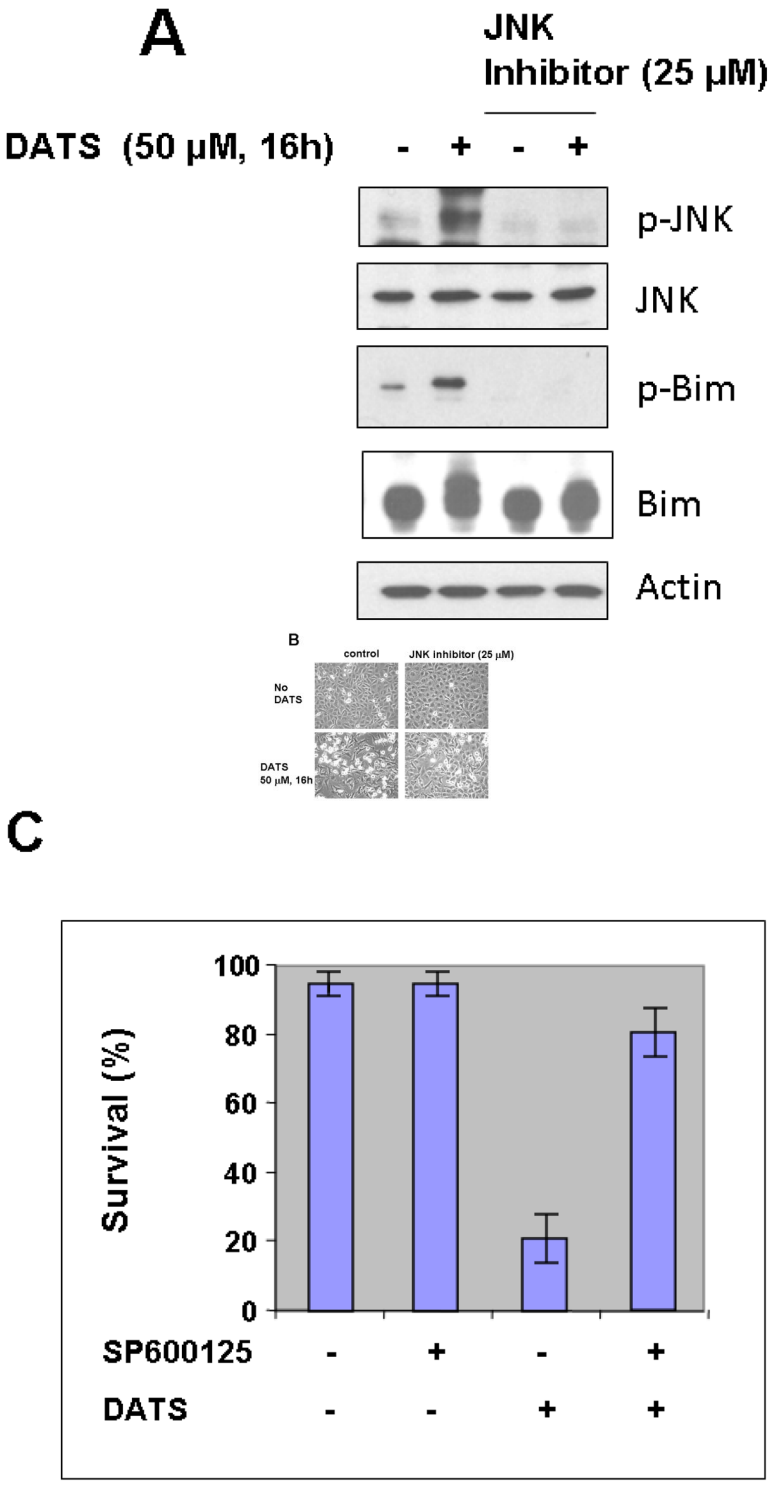

Figure 6. Effect of JNK inhibitor on DATS-induced JNK phosphorylation and cytotoxicity

MDA-MB-231 cells were pretreated with SP600125 (25 μM), a JNK inhibitor, for 30 min and then treated with DATS (50 μM) for 16 h. (**A**) Equal amounts of protein (20 μg) were separated by SDS-PAGE and immunoblotted with anti-phospho-JNK, anti-JNK, anti-phospho-Bim, and anti-Bim antibody. Actin was used to confirm that similar amounts of

proteins were loaded in each lane. (**B**) Morphological features of each cell were analyzed with a phase-contrast inverted microscope. (**C)** Survival was determined using the trypan blue exclusion assay. Error bars represent SEM from triplicate experiments.